40th Conference on Radar Meteorology, Minneapolis, MN and Online, Aug. 28 – Sep. 1, 2023

Global Assesments of Doppler Velocity Measurement Error of EarthCARE Cloud Profiling Radar Using Global Storm-Resolving Simulation

Yuichiro Hagihara, Yuichi Ohno, Hiroaki Horie (NICT), Woosub Roh, Masaki Satoh (AORI, The Univ. of Tokyo), and Takuji Kubota (EORC, JAXA)

Contact: hagihara@nict.go.jp

Short Summary:

- **The CPR on the EarthCARE satellite is the first spaceborne W-band Doppler radar.**
- **We investigated the effectiveness of horizontal integration and the unfolding method for the reduction of the Doppler error (the standard deviation of the random error) on a global scale.**
- **The error was higher in the tropics than in the other latitudes due to frequent rain echo occurrence and limitation of its unfolding correction. If we use the PRF of the low mode operation (higher PRF), the errors become small enough, although cloud echoes for altitudes higher than 16 km cannot be observed.**

Introduction

The EarthCARE is a joint satellite mission between JAXA and ESA. One of the features of this mission is the Cloud Profiling Radar (EC-CPR) with Doppler capability. Vertical Doppler velocity measurement from a moving platform suffers from broadening and folding (aliasing). We simulated pulse-pair covariances using the radar reflectivity factor and Doppler velocity obtained from a satellite data simulator and a global storm-resolving simulation (NICAM). From those covariances, we calculated the Doppler velocity including Doppler broadening and folding errors. We globally evaluated accuracy of Doppler velocities with latitudinal change of cloud and precipitation scene and with latitudinal change of pulse repetition frequency (PRF) change. Using the Level 2 algorithm, we derive horizontally integrated and unfolded Doppler velocity. Those data are compared with error-free original Doppler velocity and the standard deviation (SD) of the Doppler error are assessed for this study.

Data and Methods

- **NICAM (Satoh et al., 2008, 2014, Global Storm-Resolving model; GSRMs)**
  - ✓ Atmospheric fields: initialized with the 0.5 × 0.5 deg. ECMWF Year of Tropical Convection analysis (Waliser et al., 2012) at 00:00Z 15 June 2008.
  - ✓ Surface variables: initialized with the 1 × 1 deg. National Centers for Environmental Prediction reanalysis
  - ✓ Grid: 3.5 km in horizotal, while the vertical grid has 40 levels of grid size, ranging from 162m at the surface to 3012 m
  - ✓ Scheme: NICAM Single-moment Water 6 (NSW6) (Tomita, 2008)
- **Joint-Simulator (Hashino et al., 2013, 2016, Satellite Data Simulator)**
  - ✓ Simulate EarthCARE observations from NICAM outputs.
  - ✓ Built on Satellite Data Simulator Unit (SDSU) (Masunaga et al., 2010), specifically NASA Goddard SDSU.
  - ✓ The Z factor (Z_e) and Doppler velocity (V) are simulated by the module "EarthCARE Active SEnsor simulartor (EASE)" (Okamoto et al., 2007; 2008; Nishizawa et al., 2008).
- **L1b Data Construction**
  - ✓ Simulated data by Joint-Simulator were **then calculated along an EC orbit and interpolated into the EC-CPR sampling in-terval (100 m in the vertical and 500 m in the horizontal).**
  - ✓ **The Z factor ($Z_{e,jsim}$) and Doppler velocity (V_{jsim}) curtain data were obtained; "NICAM/J-Sim data"**
  - ✓ In this study, 16 orbits of data was used, which is equivalent to 1 d of satellite tracks.
- **Measured Velosity Simulation, Horizontal Integration, and Unfolding Methods**
  - ✓ Simulated the measured Doppler velocity (V_m)

$$V_m = V_{jsim} + V_{random}$$ ←**Add velocity error to model velocity**

  - V_{random}**: the random error caused by the spread of Doppler velocities within the beam width.** This is a Gaussian error distribution, and its SD of the random error (SD_{random}) is determined by perturbation approximation (Doviak and Zrnic, 1993). **The range of PRFs is from 6.1~7.5kHz illustrated in Fig. 1. The SD_{random} values corresponding to its max. and min. values are shown in Fig. 2.**

  - ✓ Simulated the integrated pulse-pair covariance (R_τ)

$$Re(R_\tau) = Z_{e,jsim} \cdot \cos\left(\frac{4\pi \cdot V_m}{\lambda \cdot PRF}\right)$$

$$Im(R_\tau) = Z_{e,jsim} \cdot \sin\left(\frac{4\pi \cdot V_m}{\lambda \cdot PRF}\right)$$

τ: inter pulse period (= 1/PRF),
λ: wavelength

  - ✓ Calculation of V_{500m} using 500m integrated Rτ

$$V_{500m} = \frac{\lambda \cdot PRF}{4\pi} \tan^{-1}\left\{\frac{Im(R_\tau)}{Re(R_\tau)}\right\}$$

  - ✓ 1 and 10km horizontal integration using 1 and 10km integrated Rτ
    - **To reduce random error, we conducted horizontal (along-track) integration**

$$V_{1km} = \frac{\lambda \cdot PRF}{4\pi} \tan^{-1}\left\{\frac{\sum_{1km} Im(R_\tau)}{\sum_{1km} Re(R_\tau)}\right\}$$

$$V_{10km} = \frac{\lambda \cdot PRF}{4\pi} \tan^{-1}\left\{\frac{\sum_{10km} Im(R_\tau)}{\sum_{10km} Re(R_\tau)}\right\}$$

  - ✓ Simple Unfolding method
    - From the groundbased vertically pointing cloud radar observations (Horie et al., 2000), **upward motion above 3 m/s has rarely been observed.**
    - We thus assumed that **echoes with velocities higher than 3 m/s are upward-folded precipitation echoes.**

$$V_{unfolded} = \begin{cases} V_{folded} + 2 \cdot V_{max} & \text{for } V_{1km,10km} < -3\,m/s \\ V_{folded} & otherwise. \end{cases}$$

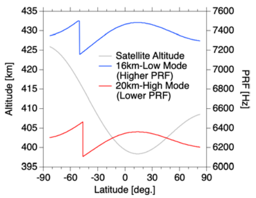

Fig.1. Satellite alt. and PRF as a function of latitude and observation window mode.

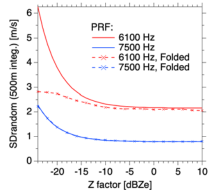

Fig.2. SD of random error for 500-m integration as a function of Z_e using the perturbation approximation method. The dashed lines denote random error considering Doppler folding.

Results and Discussion

- **Latitudinal Variation in the SD of the Random Error**
  - ✓ We **investigated the change in SD_{diff} (calc. from the diff between the simulated V_{10km} and V_{jsim}) with latitude** since the frequencies of cloud and precipitation echoes differ in latitude and the PRF varies with latitude.
  - ✓ We defined five latitudinal zones: **the Arctic (> 60°), the northern midlatitude (60 to 30°), the tropics (30 to −30°), the southern midlatitude (−30 to −60°), and the Antarctic (< −60°).**
  - ✓ We focused on the SD_{diff} of V_{10km}.

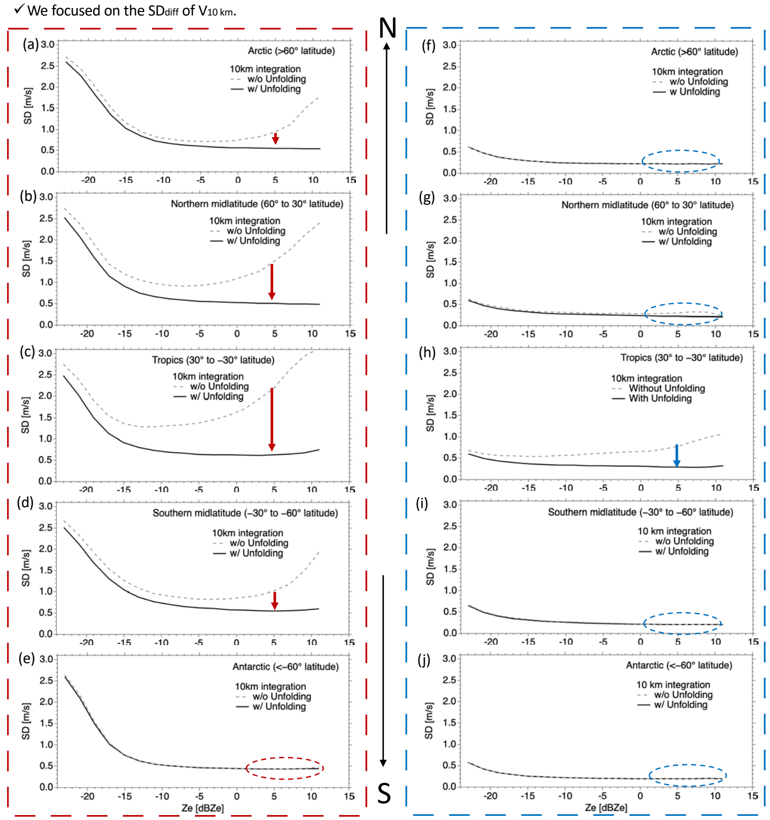

Fig. 3. SD of the random error of simulated Doppler velocities for (a–e) the PRF of the high mode (lower PRF) and (f–j) the PRF of the low mode (higher PRF) as a function of Ze after 10 km integration for (a, f) the Arctic, (b, g) the northern midlatitude, (c, h) the tropics, (d, i) the southern midlatitude, and (e, j) the Antarctic zones. The solid lines denote the results with unfolding correction.

- ✓ **20km-High mode, Lower PRF (Left panels)**
  - **The SD of V10 km w/o unfolding** decreases up to a certain value of Z_e (reduction in random error owing to the increase in the S/N and decrease in SD_{random} in Fig. 2) and increases after that value (increase in the occurrence of velocity folding & increase in the intensity of precipitation echoes and an increase in mean fall velocity). The SD for the tropics, shown in Fig. 3c, has the largest value. **The SD of V10 km w/ unfolding** decreases as Z_e increases (the folded negative velocities are corrected and the occurrence of the velocity folding is reduced).
  - From the PRF variation shown in Fig. 1, in the PRF of the high mode (lower PRF), the Doppler accuracy should be higher in the tropics and lower toward the poles. However, the results that we have seen so far show the opposite. **On the other hand, the frequency of precipitation echoes is considered to be the highest in the tropics, and the folding Doppler error may have resulted in the largest SD in the tropics.**
- ✓ **16km-Low mode, Higher PRF (Right panels)**
  - Comparison of Fig. 3a–e and 3f–j shows that the SD is much smaller in the latter (PRF of the low-mode PRF, SD_{random} is smaller (Fig.2) and the V_{max} is larger owing to the higher PRF)
  - There is a difference between w/ and w/o unfolding only for SD for the tropics (shown in Fig. 3h), which may be related to the frequency of precipitation echoes.

- **SD for the 5 latitudinal Zones for 5 dBZe**
  - ✓ To summarize what has been discussed so far, **the SD values for the five latitudinal zones for 5 dBZe were extracted** and are shown in Fig. 4.

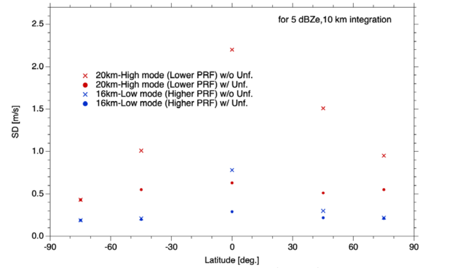

Fig. 4. SD of the random error of Doppler velocities w/ and w/o unfolding correction for 5 dBZe after 10 km integration as a function of latitude.

- ✓ **20km-High mode, Lower PRF**
  - **The SD w/o unfolding** for the tropics reached a maximum of 2.2 m/s and then decreased toward the poles. **The SD w/ unfolding** for the tropics was much smaller at 0.63 m/s.
- ✓ **16km-Low mode, Higher PRF**
  - **The SD w/o unfolding** for the tropics reached a maximum of 0.78 m/s and then decreased toward the poles. **The SD w/ unfolding** for the tropics was 0.29 m/s, which is less than half the value w/o correction.
- ✓ The latitudinal variation in the SD w/o unfolding may be due to the fre quency of precipitation echoes. **If the unfolding correction were perfect, there would be no relationship between the latitudinal variation in the SD with unfolding correction and the frequency of precipitation echoes. However, there is actually a relationship between the two, which indicates a limitation of the unfolding correction.**

- **Zonal mean frequencies of precipitation echos from NICAM/J-Sim data**
  - ✓ Freq = num of "falling" echo bins ($Z_{e,jsim}$ > −24 dBZe & V_{jsim} > 3m/s) / total num of obs. at that level. The bin size was 240 m in the vertical and 2.0° latitude in the horizontal.

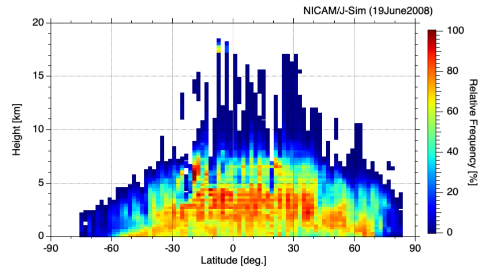

Fig. 5. Zonal mean frequency of precipitation echoes obtained by NICAM/J-Sim for 19 June 2008.

- ✓ The frequency is high in the tropics and decreases toward the poles. This is because it was summer in the Northern Hemisphere in the simulation.
- ✓ **The latitudinal variation in the SD described so far can be explained on the basis of the precipitation echo distribution.**

For more information on this poster presentation, please see the following paper: Hagihara, Y., Ohno, Y., Horie, H., Roh, W., Satoh, M., and Kubota, T.: Global evaluation of Doppler velocity errors of EarthCARE cloud-profiling radar using a global storm-resolving simulation, Atmos. Meas. Tech., 16, 3211–3219, https://doi.org/10.5194/amt-16-3211-2023, 2023.